Applied Physics Letters

Optically pumped cesium plasma neutralization of space charge in photon-enhanced thermionic energy converters

Cite as: Appl. Phys. Lett. **101**, 213901 (2012); https://doi.org/10.1063/1.4767349
Submitted: 19 July 2012 . Accepted: 29 October 2012 . Published Online: 21 November 2012

Tsuyohito Ito, and Mark A. Cappelli

Optically pumped cesium plasma neutralization of space charge in photon-enhanced thermionic energy converters

Tsuyohito Ito[1,a)] and Mark A. Cappelli[2,b)]
[1]*Center for Atomic and Molecular Technologies, Graduate School of Engineering, Osaka University, Osaka 565-0871, Japan*
[2]*Mechanical Engineering Department, Stanford University, Stanford, California 94305-3032, USA*

(Received 19 July 2012; accepted 29 October 2012; published online 21 November 2012)

Photon-enhanced thermionic emission from semiconducting cathodes is a promising means of increasing cathode current density in low temperature vacuum thermionic energy devices [J. W. Schwede *et al.*, Nature Mater. **9**, 762 (2010)]. However, the space charge resulting from high emission current densities prevents emitted electrons from reaching the collector, even with gaps as small as 100 μm and at voltages as high as 1 V. We demonstrate by particle-in-cell simulations that one possible solution to overcoming the space charge is to add cesium filling and generation of a space charge-neutralizing plasma by continuous laser excitation of the cesium resonance level.
 [http://dx.doi.org/10.1063/1.4767349]

At the center of the increase in greenhouse gas emissions, particularly CO_2 emissions, is the nearly exclusive use of carbon-based fuels in contemporary energy systems. Strategies to reducing CO_2 emissions in energy conversion systems include the utilization of renewable or carbon-free resources. Among these, systems designed directly to convert solar energy to electricity, such as photovoltaics, are the most popular due to their broad potential for deployment. Conventional, non-concentrated photovoltaics are material and capital intensive per watt because of the relatively low efficiencies (typically under 20%) and relatively low power densities (typically less than 10^2 W/m^2). Improving those metrics would reduce costs, material requirements, the scale necessary for a solar installation, and would help make solar power more cost-effective. Concentrated solar thermal technology has made much progress on this objective; however, the use of concentrators to increase power density onto energy conversion devices necessitates systems capable of conversion at higher temperatures.

It seems that concentrated solar thermionics with bottom side energy recovery affords a potential solution to the limitations often seen in solar energy conversion—more so if the thermionic energy converter (TEC) efficiency can be boosted to near ideal limits. Traditionally, thermionic energy conversion is most efficient and affords higher power densities at high temperatures (>1500 K), placing considerable challenges on the development of robust, long-life, and thermally stable emitters. In a recent study,[1] photon-enhanced thermionic emission (PETE) from semiconducting cathodes was shown to be a promising means of increasing the thermionically driven cathode current density at relatively low cathode temperatures (500-1100 K). In a semiconducting cathode, photon absorption elevates the conduction band electron density, n, above its equilibrium value, n_{eq}, increasing the effective Fermi energy (or quasi Fermi energy), $E_{F,n}$, above the Fermi energy, E_F, thereby decreasing the effective work function ($\phi_{eff} = \phi + E_F - E_{F,n}$) allowing a greater number of electrons to overcome the true work function, ϕ, and escape from the surface into vacuum. Calculations carried out in Ref. 1 indicate that a semiconductor cathode emitter with a bandgap of $E_g = 1.4$ eV and electron affinity $\chi \sim 1.0$ eV ($\phi = E_g + \chi \sim 2.4$ eV) heated to a modest 1100 K and illuminated with a concentrated (1000×) solar flux can generate a flat-line current density of almost 30 A/cm^2. When integrated into an ideal vacuum thermionic energy converter with an anode work function, $\phi_A = 0.9$ eV, and temperature of 500 K, power conversion efficiencies were seen to reach nearly 40%. These high efficiencies easily surpass those of conventional thermionic energy converters (typically 10%-15%[2,3]), which must operate at much higher temperatures (emitter temperatures well in excess of 1500 K). If combined with a means of recovering waste heat from the anode collector, the combined efficiency was shown to exceed 62%.[1] Most importantly, however, the PETE process affords an opportunity to operate thermionic converters at relatively low emitter temperatures, greatly reducing materials effects which have plagued thermionic converter development for nearly 50 years.[2,4]

At the high current densities described in Ref. 1 (3-30 A/cm^2), one might expect that the electron transport will be space-charge limited, and the majority of the electrons emitted will be returned to it because of the strong space charge electric field. We show in this letter that indeed, space charge development greatly limits the performance of the PETE thermionic converter discussed in Ref. 1. This letter also proposes a possible solution to this space-charge limitation. We propose PETE devices with cathode/anode gap distances of practical dimensions (e.g., 100 μm) and to fill the gap with cesium, as is often done with conventional thermionic converters, to serve several purposes. It serves to modify the anode work function (which, in a PETE device is typically at $T_A < 500$ K), minimized in temperature for optimum converter efficiency. Also, it serves to lower the cathode work function so that higher emission current can be obtained at the lower PETE temperatures. Finally, and perhaps most importantly, it neutralizes the space charge of the cathode-emitted electrons by producing a partially ionized plasma

[a)]tsuyohito@ppl.eng.osaka-u.ac.jp.
[b)]cap@stanford.edu.

through contact ionization with the hotter cathode. However, in a PETE device, the photoelectron excitation process is specifically intended to reduce the cathode temperature requirement and the usual contact ionization alone will not suffice at these lower cathode emitter temperatures (<1100 K) to maintain a sufficiently high plasma density. Therefore, in this letter, we propose the lowering of the cesium effective ionization potential by photo-exciting the electronic (6^2P) energy state (resonance state) at 1.39 eV. In this way, a significant degree of Cs ionization will occur at lower cathode temperatures by electron collisional ionization and plasma densities will be sufficiently high to adequately neutralize space charge. This resonance-enhanced PETE (or R-PETE) process is examined computationally using particle-in-cell (PIC) simulations, below.

It is well known that the cesium filling of the gap to produce plasma may also introduce some collisions between the anode-bound (cathode emitted) electrons and cesium particles resulting in an additional loss that can diminish overall converter performance. This loss (barrier loss) is common in high temperature, so-called "ignited" (plasma-forming) cesium thermionic converters, and must be accounted for in any practical Cs-filled converter performance analysis. In order to evaluate the performance of this complex cesium-filled PETE converter, we employ PIC simulations. In PIC simulations,[5] the motion of discrete negative, positive, and neutral superparticles (each representing a finite number of the electrons, positive ions, and neutral atoms, respectively, in the gap) is tracked according to the electrostatic forces that push them. Direct simulation Monte Carlo (DSMC) methods are used in conjunction with PIC to randomize particle velocities and directions due to the possibility of momentum-exchange and energy-exchange collisions, and to produce electron-ion pairs as a result of electron impact ionization of neutral cesium. The electric fields (and hence electric potential within the gap) are computed self-consistently by calculating the instantaneous local electron and ion number density (a result of tracking the location of these superparticles) on a computational grid, and using these densities to solve Poisson's equation. The computed fields are then used to push the particles and the problem advances in time in an explicit manner starting from some initial state until steady state is achieved.

The model that we have developed is one dimensional in physical space and tracks velocities in three dimensions (so-called 1D-3V PIC). The simulation assumes two parallel physical boundaries (of infinite extent—the emitter and collector). A non-uniform computational grid spacing is used to solve for the potential, providing higher resolution near the emitter where the electron density is maximum in most conditions and large potential drops can take place due to space charge formation.

As an initial study using this PIC method, direct electron emission from the cathode emitter (vacuum PETE) can be simulated in accordance with the PETE specifications under modest cathode temperature conditions described in the supplement to Ref. 1, i.e., for emitter temperatures and work functions 673 K and 1.9 eV, respectively. The anode temperature and work functions are 573 K and 0.9 eV, respectively. The work function reduction by photon enhancement is 0.93 eV, resulting in an "effective" work function of 0.97 eV. Under these conditions, Ref. 1 computes a photon-enhanced thermionic emission current density of 3 A/cm^2. A short circuit will lead to a favorable (1V) voltage across the gap that will attract the cathode-emitted electrons. The results of PIC simulations for a vacuum gap distance of 100 μm are shown in Fig. 1. The left boundary represents the cathode emitter, while the right is the anode collector. Shown in the figure is the electron number density as a red broken line and the potential (relative to the collector) as blue solid line. The anode potential is positive 1 V relative to the cathode, as expected for the short-circuit conditions and the specified work functions. An apparent feature of this simulation is the large space charge that develops in the vicinity of the emitter that generates a potential that is more negative than the cathode by more than half a volt. It is noteworthy that the higher temperature conditions discussed in Ref. 1 will result in an even stronger space charge potential. This potential well repels incident electrons from the left boundary (cathode) and pulls back electrons emitted from the low-work function anode (right boundary) resulting in increased densities near the two electrodes. The scale over which these densities increase are the Debye layers, which are approximately $\lambda_D = 2$ μm thick. The electron bunching at the emitter results in an increase in the electron density by more than an order of magnitude above what would be expected in the absence of space charge. The computed vacuum current density is 0.15 A/cm^2, less than 5% of that which is emitted, i.e., about 5% the ideal limit.

For simulating the R-PETE characteristics, cesium particles are added to the simulation. The added particles are now neutral cesium in the ground, $6S_{1/2}$ electronic state (Cs), neutral cesium in its electronically excited $6P_{1/2,3/2}$ state (Cs*) at 1.39 eV, and cesium ions (Cs^+). The related cesium energy level diagram and transition processes are shown schematically in Fig. 2. The total number density of cesium (sum of Cs, Cs*, and Cs^+) is kept constant during the simulation, although the weight of the superparticles may be

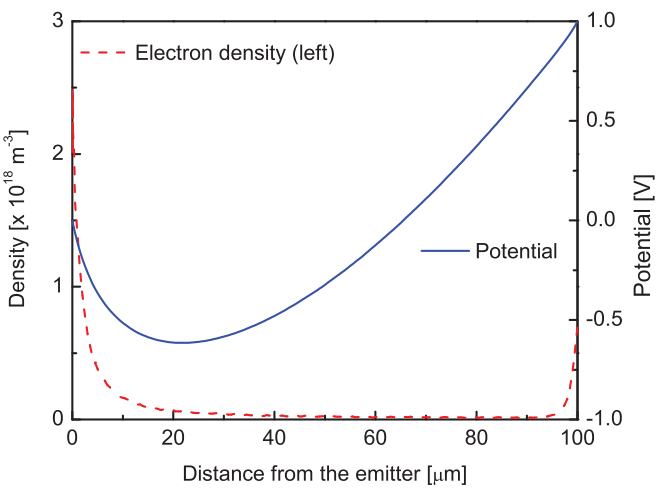

FIG. 1. Electron density (red broken line) and potential distribution (blue solid line) for the vacuum PETE converter with the gap length of 100 μm. The gap voltage $V_g = 1$ V. The temperatures and the work functions are 673 K–1.9 eV for the emitter and 573 K–0.9 eV for the collector. Work function reduction by photon enhancement is 0.93 eV, resulting in an "effective" work function of 0.97 eV. The current output is 1.5 kA·m^{-2}.

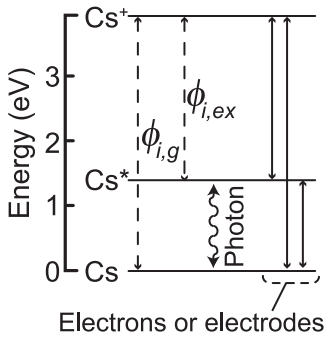

FIG. 2. Cesium energy level diagram and photoexcitation process.

different. Molecular dimers are not considered at this time as they are expected to be much lower in number. The Cs, Cs*, and Cs^+ are modeled to collide with the emitter and/or collector and can lead to ionization, as specified by the appropriate cross sections for these elementary processes described below. Electrons (electrode emitted or generated via ionization) tracked through the gap are allowed to gain energy via Joule heating, and lose energy through collisions with the cesium particles (Cs, Cs*, and Cs^+) based on their density distributions. We assume that electron capture at the collector occurs with unity probability. Excitation, ionization, superelastic, and recombination collisions are considered for electron-heavy particle collisions. The cross sections for excitation and ionization from the ground state are taken from Ref. 6, ionization cross section from the excited state is based on the Drawin formula,[7] and the cross section for superelastic collisions is estimated based on the principle of detailed balancing. The scattering angle and partitioning of energies following collisions are defined as described in Ref. 8 by using an appropriate differential cross section for elastic collisions[8,9] and the energy partition function for ionization with the spectrum sharp parameter[8,10] of 4 eV. The excitation and superelastic collisions are also treated as is described in Ref. 8. The recombination probability is computed in accordance with the method described by Momozaki and El-Genk[11] using an electron-ion binary collision rate of 5.3×10^{-13} m^3/s and we assume that recombination creates a ground-state neutral cesium at the same position with a velocity equal to that of the recombining ion. Ion-neutral particles' collisions are accounted for by including charge exchange collisions (cross sections of 6×10^{-18} m^2 for both Cs and Cs*) and isotropic scattering (10^{-18} m^2 cross section). Neutral-neutral particle collisions are assumed to have the same isotopic scattering cross section as that of ion-neutral scattering (10^{-18} m^2). The photoexcitation process generating excited cesium is included by specifying the fraction of excited state cesium, i.e., $N_{ex}/(N_{ex}+N_g)$. Here, N_{ex} is the number of excited Cs* atoms, while N_g is the number of ground state cesium atoms, Cs. In theory, with sufficiently high laser fluence, the ratio $N_{ex}/(N_{ex}+N_g)$ can be as high as 0.75 when the resonance levels are saturated, although the overall energetics of the process will be strongly related to the ability for the laser to maintain saturation with negligible resonance radiation escape.

The modeling of the contact ionization requires some consideration of the effect of the external photoexcitation of the emitter as specified by the PETE process. As mentioned earlier, this photoexcitation produces holes in the valance band and elevated numbers of electrons in the conduction band. This enhancement is equivalent to that which can be achieved at a much higher temperature. To model the contact ionization, we use the emitter temperature-dependence specified in the Saha-Langmuir equation,[12] but employ an effective temperature equal to that necessary to produce the thermionic electron emission from the metal cathode with a work function of 1.9 eV (1265 K for 3 A/cm^2). Using again conditions typical of the PETE process described in the supplement of Ref. 1 that leads to relatively high emitter current densities (3 A/cm^2), we have simulated the cesium-filled ignited PETE converter behavior for a range of cesium excitation fractions, $N_{ex}/N_{ex}+N_g$, two initial cesium fill conditions (0.2 and 1 Torr at 573 K), and for a short-circuited converter with $V_g = 1$ V. The vapor pressure of Cs at 573 K (the lowest electrode temperature wall in our system) is approximately 1.9 Torr (250 Pa), which is higher than the fill conditions.

These results are shown in Fig. 3. We see from Fig. 3 that by varying the excitation fraction, we can span the entire range of current density defined by the vacuum PETE process. The upper range of current densities possible is limited by the PETE enhanced thermionic emission at the emitter, 3 A/cm^2 for the conditions given (in the caption), whereas the lower limit is defined by the space-charge limited flow in vacuum shown in Fig. 1, i.e., about 0.15 A/cm.[2]

We see from Fig. 3 that at low excitation fractions, the plasma density is not sufficient to neutralize the space charge and the current density collected at the anode is close to that of the space charge vacuum limit. At high excitation fractions, the current densities approach the theoretical PETE thermionic emission limits (for the 1 Torr fill condition). The

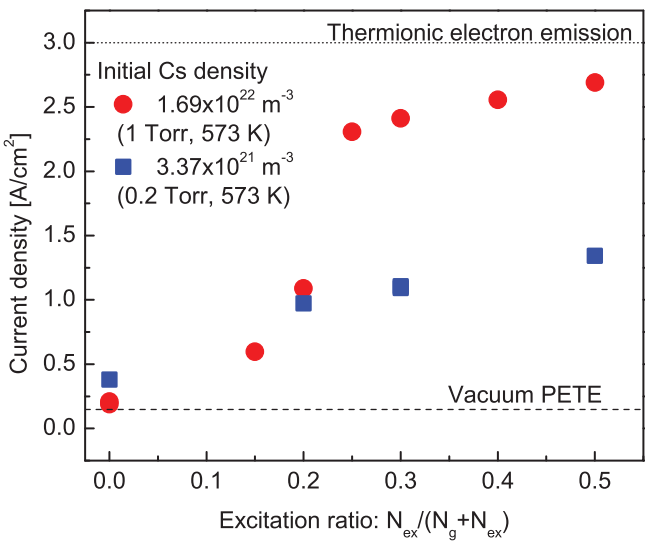

FIG. 3. Computed current density for initial cesium fill density of 1.69×10^{22} m^{-3} (corresponding to the ideal gas density of 1 Torr-573 K) and 3.37×10^{21} m^{-3} (0.2 Torr, 573 K) with the gap voltage of 1 V corresponding a short circuit (0 output voltage). The emitter and collector temperatures are 673 K and 573 K. ϕ_E and ϕ_C are 1.9 eV and 0.9 eV, respectively. Also shown as the broken and dotted lines corresponding to ideal thermionic electron emission current density and the space charge limited vacuum current density.

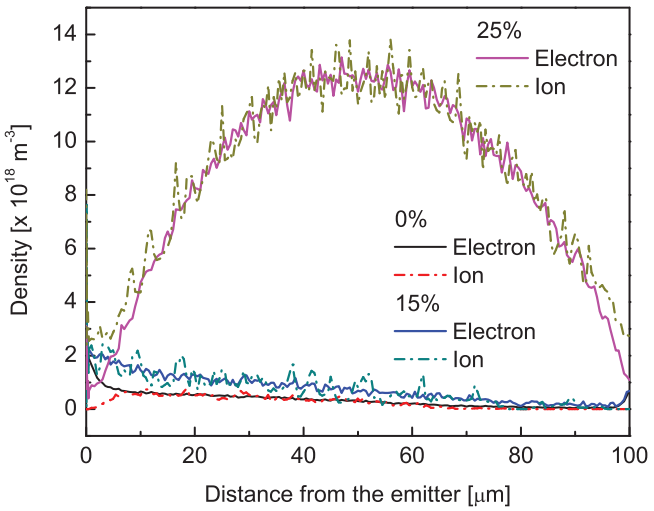

FIG. 4. Electron and ion density distributions for the Cs density of 1.69 $\times$ 10^{22} m^{-3} (1 Torr, 573 K) with the gap voltage of 1 V (short circuit) for several excitation ratios $N_{ex}/(N_g + N_{ex})$, which are shown in the legend.

sudden rise in current is due to the thermionic converter ignition, i.e., the rapid rise in plasma density associated with superelastic heating and runaway ionization. The computed electron and ion number densities within the R-PETE gap are shown in Fig. 4, for excited state excitation fractions of 0%, 15%, and 25%. Figure 5 shows the potential distribution for the excitation fractions of 0%, 15%, 20%, and 25%. Here, we see that the strong space charge that exists at 0% (difference between the red and the black curves, near the emitter in Fig. 4, as well as the negative potential in Fig. 5) virtually disappears at 15% excitation with only a modest increase in overall plasma density. While the plasma density at an excitation fraction of 20% (not shown) is only slightly higher than that at 15%, the density is seen to increase dramatically at 25%.

These results confirm that a vacuum PETE device constructed with practical gap spacings (e.g., 100 μm) cannot perform at its theoretical limit due to space charge formation within the gap. To avoid space charge limitations, the gap would have to be of order the Debye length in separation, typically about a few microns in scale. Equally important is that the results also show that cesium fill without excitation of the cesium cannot generate the plasma density needed to neutralize the space charge in the examined conditions. Finally, the results demonstrate that with resonance state excitation of the cesium and sufficient fill pressure, near theoretical limits in current density are possible. However, this is only achieved at high excitation fractions, above 25%.

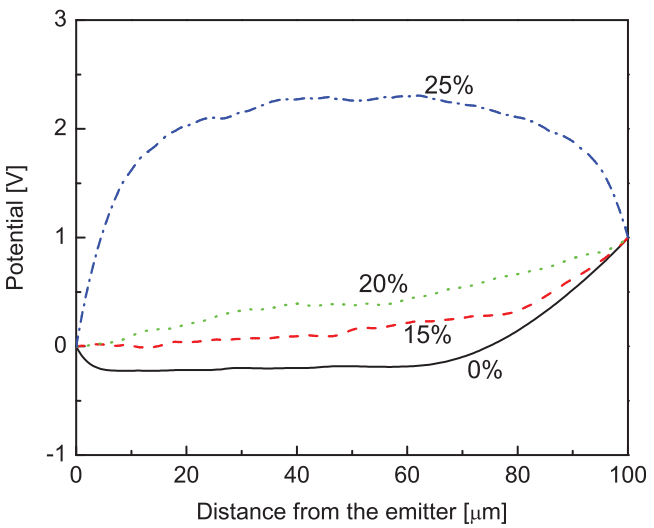

FIG. 5. Potential distributions for the Cs density of 1.69 $\times$ 10^{22} m^{-3} (1 Torr, 573 K) with the gap voltage of 1 V (short circuit) for several excitation ratios $N_{ex}/(N_g + N_{ex})$, which are shown in figure.

The above calculations were carried out for short-circuited converters. The computed current density versus output voltage for a Cs-filled PETE converter shows that at 30% excitation fraction at the 1 Torr initial fill condition, a load voltage of 0.8 V will produce an output power density of 1.2 W/cm^2, approximately half of the theoretical PETE limit. Of course, the short circuit current density is within 80% of the theoretical limit, but it produces no output power.

While the enhancement in performance seen with photo-excitation of the cesium resonance electronic state seems to be encouraging, at this time we do not model the radiative excitation and de-excitation explicitly, and in particular, the radiation diffusion and loss from the plasma between the electrodes. As a result, we cannot, at this time, assess the overall system energetics. We also note that we do not model the possible presence of molecular dimers or dimer ions, and so associative ionization mechanisms are not yet included in the simulations. These additional ionization processes will only improve the overall ability of the laser-excited Cs to neutralize the space charge. The absence of associative ionization may explain in part why the model requires the artificial introduction of an approximately 20% excited state population to match the current density reported in Fig. 8 of Ref. 3 for a conventional TEC with an emitter temperature of 1700 K. We also note that the interaction of Cs with such high temperature emitters is still poorly understood in that ionization can also arise by contact excitation of Cs followed by associative ionization, further enhancing the overall effective contact ionization process. Despite the need for refinements to the simulations to account for these surface processes, this letter has demonstrated the importance of the neutralization of the space charge in PETE converters, and has introduced resonance excitation as a means of increasing the overall output current densities. Future research will focus on the overall energetics accounting for resonance radiation loss.

This research has been supported in part by the Global Climate and Energy Project (GCEP) at Stanford University and the Japan Society for Promotion of Science (JSPS)/the Japan Ministry of Education, Culture, Sports, Science and Technology (MEXT).

[1]J. W. Schwede, I. Bargatin, D. C. Riley, B. E. Hardin, S. J. Rosenthal, Y. Sun, F. Schmitt, P. Pianetta, R. T. Howe, Z.-X. Shen, and N. A. Melosh, Nature Mater. **9**, 762, (2010).
[2]G. N. Hatsopoulos and E. P. Gyftopoulos, *Thermionic Energy Conversion* (MIT, 1973), Vol. I.
[3]N. S. Rasor, IEEE Trans. Plasma Sci. **19**, 1191 (1991).
[4]A. V. Da Rosa, *Fundamentals of Renewable Energy Processes* (Elsevier Academic, 2005).
[5]C. K. Birdsall and A. B. Langdon, *Plasma Physics via Computer Simulations* (Taylor and Francis Group, 2005).

[6]A. Zecca, G. P. Karwasz, and R. S. Brusa, Riv. Nuovo Cimento **19**, 1 (1996).
[7]M. Mitchner and C. H. Kruger, Jr., *Partially Ionized Gases* (Wiley Interscience, New York, 1973).
[8]V. Vahedi and M. Surendra, Comput. Phys. Commun. **87**, 179 (1995).
[9]M. Surendra, D. B. Graves, and I. J. Morey, Appl. Phys. Lett. **56**, 1022 (1990).
[10]C. B. Opal, W. K. Peterson, and E. C. Beaty, J. Chem. Phys. **55**, 4100 (1971).
[11]Y. Momozaki and M. S. El-Genk, J. Appl. Phys. **92**, 690 (2002).
[12]M. J. Dresser, J. Appl. Phys. **39**, 338 (1968).